AD-A125 611 COMPUTER MODELING OF SIMPLE POINT DEFECTS IN RARE EARTH 1/1
DOPED ALKALINE EARTH FLUORIDES(U) NAVAL ACADEMY
ANNAPOLIS MD DEPT OF PHYSICS J J FONTANELLA ET AL.
UNCLASSIFIED 01 JUL 82 TR-4 F/G 9/2 NL

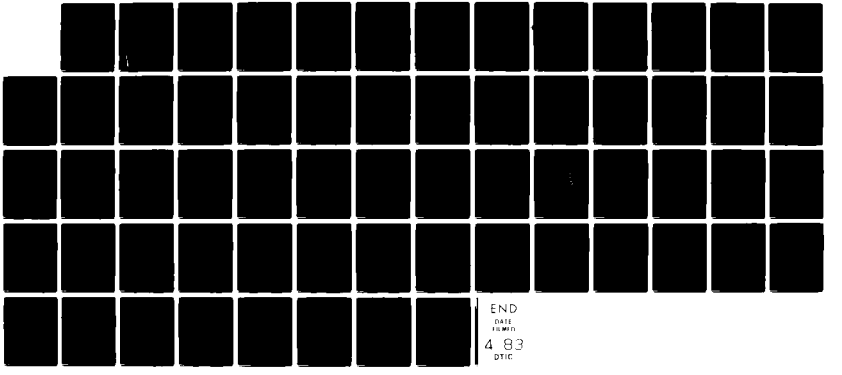

END
DATE FILMED
4 83
DTIC

M-2

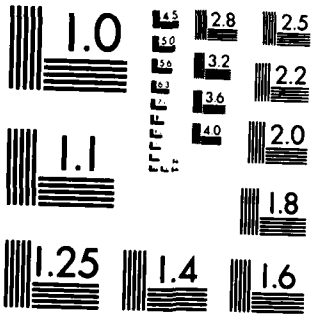

MICROCOPY RESOLUTION TEST CHART
NATIONAL BUREAU OF STANDARDS 1963 A

(12)

OFFICE OF NAVAL RESEARCH

Contract N00014-82-AF-00001

Task No. NR 627-793

TECHNICAL REPORT NO. 4

Computer Modeling of Simple Point Defects in Rare Earth Doped Alkaline Earth Fluorides

by

John J. Fontanella and Mary C. Wintersgill

Prepared for Publication

in the

Journal of Physics C: Solid State Physics

U. S. Naval Academy
Department of Physics
Annapolis, MD 21402

July 1, 1982

SECURITY CLASSIFICATION OF THIS PAGE (When Data Entered)

REPORT DOCUMENTATION PAGE

READ INSTRUCTIONS BEFORE COMPLETING FORM

1. REPORT NUMBER: 4	2. GOVT ACCESSION NO.
3. RECIPIENT'S CATALOG NUMBER	
4. TITLE (and Subtitle): COMPUTER MODELING OF SIMPLE POINT DEFECTS IN RARE EARTH DOPED ALKALINE EARTH FLUORIDES	5. TYPE OF REPORT & PERIOD COVERED: Interim Technical Report
	6. PERFORMING ORG. REPORT NUMBER
7. AUTHOR(s): R.J. KIMBLE, JR., P.J. WELCHER, J.J. FONTANELLA, M.C. WINTERSGILL; C.G. ANDEEN,	8. CONTRACT OR GRANT NUMBER(s): N0001482AF00001
9. PERFORMING ORGANIZATION NAME AND ADDRESS: U. S. Naval Academy, Physics Department, Annapolis, Maryland 21402	10. PROGRAM ELEMENT, PROJECT, TASK AREA & WORK UNIT NUMBERS: NR No. 627-793
11. CONTROLLING OFFICE NAME AND ADDRESS: Office of Naval Research, Attn: Code 413, 800 N. Quincy St., Arlington, VA 22217	12. REPORT DATE: July, 1982
	13. NUMBER OF PAGES: 53
14. MONITORING AGENCY NAME & ADDRESS(if different from Controlling Office)	15. SECURITY CLASS. (of this report)
	15a. DECLASSIFICATION/DOWNGRADING SCHEDULE

16. DISTRIBUTION STATEMENT (of this Report)

Approved for public release and sale.
Distribution unlimited.

17. DISTRIBUTION STATEMENT (of the abstract entered in Block 20, if different from Report)

18. SUPPLEMENTARY NOTES

Journal of Physics C: Solid State Physics, to be published.

19. KEY WORDS (Continue on reverse side if necessary and identify by block number)

solid electrolytes, fluorine ion conductors, point defects, computer calculations

20. ABSTRACT (Continue on reverse side if necessary and identify by block number)

The results of a package of FORTRAN computer programs for modeling defects in ionic crystals and for fitting experimental data are described. The fundamental concept of the defect simulation is similar to HADES except that the minimization procedure is different since the package is designed to run on small computers. As an example of the use of this package, the relative stabilities of nn and nnn complexes for various rare earths, lanthanum, and yttrium are considered.

(Continued on reverse side)

DD FORM 1 JAN 73 1473 EDITION OF 1 NOV 65 IS OBSOLETE
S/N 0102-014-6601

SECURITY CLASSIFICATION OF THIS PAGE (When Data Entered)

20. Abstract

First, the data fitting routine was used to analyze relaxation data for nn and nnn complexes in rare earth doped strontium fluoride. The experimental results for strontium fluoride were then used in conjunction with the defect simulation program to determine potentials for all of the rare earths, yttrium, and lanthanum. Those rare earth potentials were then used in the simulation of calcium fluoride and show that the nnn complex should not be observable except for possibly the smallest rare earths. This implies that the B site of Wright and co-workers or the RII relaxation requires another explanation. Also, the potentials were used in the simulation of barium fluoride, showing that the nn complex should be observable only for the largest rare earths or lanthanum. Next, the enthalpy for nn→nn reorientation via the interstitialcy mechanism was calculated for rare earths in calcium and strontium fluoride. In general, the calculated reorientation enthalpies are larger than the experimental values. However, the variation of the enthalpy with the size of the rare earth is in reasonable agreement with experiment. Finally, the variation of the calculated enthalpy with pressure is found to be in excellent agreement with experiment.

Computer Modeling of Simple Point Defects in Rare Earth Doped Alkaline Earth Fluorides

Robert J. Kimble, Jr. and Peter J. Welcher

Mathematics Department

U. S. Naval Academy

Annapolis Md. 21402, USA

and

John J. Fontanella and Mary C. Wintersgill

Physics Department

U. S. Naval Academy

Annapolis Md. 21402, USA

and

Carl G. Andeen

Physics Department

Case Western Reserve University

Cleveland, Ohio 44106, USA.

Abstract

The results of a package of FORTRAN computer programs for modeling defects in ionic crystals and for fitting experimental data are described. The fundamental concept of the defect simulation is similar to HADES except that the minimization procedure is different since the package is designed to run on small computers. As an example of the use of this package, the relative stabilities of nn and nnn complexes for various rare earths, lanthanum, and yttrium are considered. First, the data fitting routine was used to analyze relaxation data for nn and nnn complexes in rare earth doped strontium fluoride. The experimental results for strontium fluoride were then used in conjunction with the defect simulation program to determine potentials for all of the rare earths, yttrium, and lanthanum. Those rare earth potentials were then used in the simulation of calcium fluoride and show that the nnn complex should not be observable except for possibly the smallest rare earths. This implies that the B site of Wright and co-workers or the RII relaxation requires another explanation. Also, the potentials were used in the simulation of barium fluoride, showing that the nn complex should be observable only for the largest rare earths or lanthanum. Next, the enthalpy for nn→nn reorientation

via the interstitialcy mechanism was calculated for rare earths in calcium and strontium fluoride. In general, the calculated reorientation enthalpies are larger than the experimental values. However, the variation of the enthalpy with the size of the rare earth is in reasonable agreement with experiment. Finally, the variation of the calculated enthalpy with pressure is found to be in excellent agreement with experiment.

1. Introduction

In the past few years, the authors have been studying defects in ionic crystals (Andeen et al, 1981; Andeen et al, 1977), using dielectric relaxation techniques. The relaxation spectra of many systems previously thought to be quite simple, are found actually to be very complex. For example, seven relaxations are observed in rare earth doped calcium fluoride (Andeen et al. 1981).

In order to aid in the interpretation of the data, the authors have developed computer simulation techniques similar to the HADES (Harwell Automated Defect Evaluation System) program, which has produced many significant results (Catlow, Norgett, and Ross 1977; Catlow 1976). The main concept is to model a crystal by a central region of movable ions surrounded by a dielectric continuum. Shell model potentials are used for the movable ions. Defects may then be introduced into the central region after which the ions are allowed to relax to their minimum energy configuration. However, the difficulty with HADES is that the storage requirements are great, requiring a very large and fast computer. Consequently, the authors have developed an alternative package which requires far less storage with only a modest increase in the running time, making it suitable for more

general use.

The particular system used by the authors has the additional feature that all output may be displayed on an Evans and Sutherland Picture System. Stereographic display is available to enhance the three-dimensional effect. Movie-making facilities also tie in with the picture display.

As a related application of the minimization procedure associated with the computer simulation, a program for the least-squares fitting of data has also been developed. In the example presented in this paper, both techniques are used to study simple point defects in rare earth doped alkaline earth fluorides.

2. The Programming Technique

The key feature in computer programs of this type is, of course, the minimization procedure. In the case of data fitting, the sum of the squares of the differences between the data and the best-fit curve is minimized. In simulating a defective solid, the energy of the central region will be minimized. The following brief discussion of the minimization procedure will be in terms of the defect simulation. A similar technique is used in data fitting, where adjustments are made in the fitting parameters rather than ion positions.

In the present program, a modified block quasi-

Newton method (Rheinboldt 1974) is used. By block, we mean an iterative approach, where the position of each ion is adjusted, one at a time. This is the analogue of the Gauss-Seidel procedure for solving a linear system. The position of each ion is represented by six variables, three nuclear and three shell coordinates. A standard Newton-Raphson method is used to determine a new location for the chosen ion, except that for stability of the algorithm, and as a safeguard against local minima, the energy is evaluated at eight positions nearby. These values are used to approximate the derivatives called for in the Newton-Raphson technique. There are, of course, risks involved in numerical approximation of derivatives and great care is taken to avoid the pitfalls.

However, convergence using this procedure is slow. Thus, the procedure was modified to evaluate the potential function twice in the direction of the Newton-Raphson step, at the Newton distance and at half that. Fitting to a parabola determines much more accurately the minimum in this direction. As a check, the energy is evaluated once more at the location determined by the parabolic fitting. The ion is moved to the position at which the energy was least. This provides a safeguard against error in the numerical approximation of derivatives. R-linear convergence

(Rheinboldt 1974) is expected and this has been observed.

Symmetry is not invoked in our minimization and thus configurations of low symmetry are easily dealt with by the current program.

The most important feature of the present implementation is that the program requires only 18,500 36-bit words together with the ability to perform double precision computations in FORTRAN. This, combined with the efficient minimization procedure makes the program suited to small computers.

In the case of data fitting, at first inspection it might appear that a more efficient minimization technique such as that of Broydon or Fletcher-Powell would be more desirable since the storage requirements would be small. However, the present technique does not require calculation of the derivative of the function to be fit. In addition, the difference in times involved in minimization by the different techniques is small because of the the number of variables involved. Finally, the fits are done in an iterative manner and the resultant graphical display provides added evidence of the goodness of fit.

Consequently, the minimization technique employed in the defect simulation was also applied to the data fitting.

Further details of the techniques are given in Appendices A-C.

3. Defect Simulations

We now give further details of the operation of the defect simulation package. The model contains about 150 movable ions (5x5x5 fluorines plus appropriate cations). These are "surrounded" by a continuum of fixed ions, each of which is assigned a total (electronic plus ionic) polarizability. The electrostatic calculations for a given ion in the central region are performed exactly for the surrounding cube of 11x11x11 fluorines plus cations. The remaining electrostatic energy is approximated via a Madelung sum.

One or more defect ions can be added to a computer file containing the basic model including substitutionals, interstitials, or vacancies. The lattice is then allowed to relax to the minimum energy configuration as described in the previous section.

The energy of a given ion is the sum of five terms, E=ESP+ES+EN+ENR+ENR2. The spring energy, ESP, is due to the relative positions of the nucleus and

shell. The shell component of the electrostatic energy is ES and EN is the nuclear component. The near neighbour repulsive interaction, ENR, is given by summing the potentials A exp(-r/ ρ) over the nearest neighbours of the ion being moved. A and ρ are constants depending on the ions involved. The second neighbour interactions, ENR2, are included in exactly the same manner as by Catlow et al. (1977).

The distance between ions is limited to be no smaller than 1.25 times one lattice unit (defined as half the average fluorine-fluorine distance), so as to prevent computational instability in the form of two ions "collapsing together." In each case the program searches for the two ions having the smallest separation after final convergence. In no case have the two closest ions been near 1.25 lattice units apart, implying that the arbitrary repulsion has not affected the results.

In the present model, the continuum polarization was not included in the minimization procedure. Certainly, this has little effect in the case of neutral defects. However, in order to evaluate the magnitude of this effect, the polarization energy was calculated after minimization, as follows.

The excess charge, Q, and dipole moment, $\underset{\sim}{P}$, of the central movable region was evaluated. Then the

energy of each ion was set equal to:

$$W_i = -\frac{\alpha_i(\varepsilon'-1)}{\alpha\,(4\pi\varepsilon')^2\varepsilon_o N r^6}\{Q^2r^2+4PQr(\cos 0)+P^2+3P^2\cos^2\theta\} \quad (1)$$

where ε' is the static dielectric constant and N is the number of molecules per unit volume. This is essentially a modified Mott-Littleton (1938) approach since the polarizabilities, defined by:

$$\frac{\varepsilon'-1}{\varepsilon'+2} = \frac{N\alpha}{3\varepsilon_o} \quad (2)$$

and

$$\alpha = \alpha_{anion} + 2\alpha_{fluorine} \quad (3)$$

include both electronic and ionic polarizabilities. Further, the polarizabilities were separated using the empirical result that:

$$\frac{V}{\kappa_T}\left(\frac{\partial\alpha}{\partial V}\right)_T = 1 - \frac{3}{\kappa_T(\varepsilon'-1)(\varepsilon'+2)}\left(\frac{\partial\varepsilon'}{\partial P}\right)_T \approx 2 \quad (4)$$

where κ_T is the isothermal compressiblity. This result is known as the Jarman rule (Gibbs and Jarman 1962) and the experimental results for the alkaline earth fluorides using the data of Andeen et al. (1972) are listed in table 1. Also listed there are the values for some other ionic crystals using the data of Fontanella et al. (1972). It is seen that the

above relation holds quite well. Since equation [4] implies that:

$$\alpha = (\text{Constant})V^2$$

it is assumed that:

$$\alpha = (\text{Constant})R^6$$

Using the ionic radii of Shannon (1976), a set of polarizabilities was calculated and these are listed in table 2.

4. Simple Point Defects in Rare Earth Doped Alkaline Earth Fluorides

4.1. Data Fitting

Simple point defects in rare earth doped strontium fluoride provide an excellent case in which to apply data fitting and defect simulation techniques. This can be seen in figure 2 of a previous paper (Andeen et al. 1981) where it is seen that for strontium fluoride the ratio of the two principal peaks varies smoothly with a change in the size of the rare earth. What is not apparent is that in cases where both peaks exist simultaneously, they are in thermal equilibrium with one another. This is clearly shown in figure 1 where the results for gadolinium doped strontium fluoride are plotted. It is seen that the

height of the higher temperature peak actually increases with temperature while the height of the lower temperature peak decreases faster than expected on the basis of Curie-Weiss behaviour. This implies that the higher temperature peak grows at the expense of the lower temperature peak. This problem has, of course, been solved by Matthews and Crawford (1977) who explain their ITC data for gadolinium doped strontium fluoride by assigning the peaks to jumps of nn and nnn dipoles. They assign an enthalpy difference:

$$\Delta E_{12} = E_{12} - E_{21}$$

to the difference in binding energies of the two complexes. This corresponds to the enthalpies shown in figure 2, and ΔE_{12} will be a key parameter in the following discussion.

The model of Matthews and Crawford was applied to the data in the following manner. Firstly, Cole-Cole expressions were used to approximate the relaxation peaks leading to:

$$\varepsilon'' = \sum_{i=1}^{2} \frac{A_i \cos(\alpha_i' \pi/2)}{2T\{\cosh((1-\alpha_i')x_i) + \sin(\alpha_i' \pi/2)\}} \qquad (5)$$

where

$$x_i = \ln(\omega(\tau_o)_i \exp(E_{i1}/kT)) \qquad (6)$$

α_i' is the Cole-Cole parameter and is a measure of the broadening of the peaks. The use of E_{11} and E_{21} follows from the approximation

$$E_{11} > E_{12} \text{ and } E_{21}$$

as shown by Matthews and Crawford (1977). The $(\tau_o)_i$ are the so-called reciprocal frequency factors. Also,

$$A_i = \frac{N_i P_i^2}{3\varepsilon_o k}$$

where N_i is the dipole concentration and P_i is the dipole moment. It follows that:

$$\frac{N_2}{N_1} = \exp(\Delta S_{12}/k - \Delta E_{12}/kT) \qquad (7)$$

Conserving the total number of dipoles:

$$N_1 + N_2 = N_T$$

therefore:

$$A_1 = \frac{C_1}{\{1+\exp(\Delta S_{12}/k - \Delta E_{12}/kT)\}} \qquad (8)$$

and

$$A_2 = \frac{C_2}{\{1+\exp(\Delta E_{12}/kT - \Delta S_{12}/k)\}} \qquad (9)$$

Consequently, the theoretical expression given by the above equations contains ten adjustable parameters,

$$C_i,\ E_{i1},\ \alpha_i',\ \Delta S_{12},\ \Delta E_{12}$$

This is, of course, a large number of parameters. However, it should be remembered that effectively ten peaks are being fitted simultaneously since there are two different relaxations with five curves (frequencies) for each. (Only three are shown in figure 1.)

The results of the two peak data analysis are given in table 3 for the central four rare earths. A typical best fit curve is shown with the data in figure 1. The value of ΔE_{12} for gadolinium, 0.058 eV, is slightly larger than the values 0.046, 0.049, and 0.044 eV reported by Matthews and Crawford (1977), Fontanella et al. (1978a), and Edgar and Welsh (1979), respectively. However, they probably agree to within a reasonable error. The value of 0.08 eV for europium is close to 0.078 eV reported by Fontanella et al. (1978a). The other values are new. The peaks for the other materials were determined using single peak fits to equation (5).

4.2. Computer Simulations

4.2.1. Defect Stabilities

The computer simulation was then applied to the same problem. The interionic potentials are the same as those used by Catlow et al. (1977). As an initial test of the model, a substitutional trivalent rare earth was modelled merely by adjusting the shell charge of the calcium ion, in the same way that Catlow (1976) did. In this approximation, it was found that

$$(\Delta E_{12})_{TH} = -0.11 \text{ and } -0.31 \text{ eV}$$

for calcium and strontium fluoride, respectively. These values are in reasonable agreement with the values of

$$(\Delta E_{12})_{TH} = -0.03 \text{ and } -0.4 \text{ eV}$$

determined by Catlow (1976) using the HADES model. In part, the small difference is due to the polarization of the continuum. However, the important result is that the theoretical values are much lower than the experimental values listed in table 3 since the values for Tb-Sm are all positive. Since the value of $(\Delta E_{12})_{EXP}$ decreases as the size of the rare earth decreases, it was concluded that the error in the theoretical calculation was with the rare earth potential, the effective ionic radius being too small.

The simplest approach was taken to simulate larger trivalents, namely, the pre-exponential in the expression for the near-neighbour interaction

$$V(r) = A \exp(-r/\rho)$$

was increased. The results of the calculations for relative binding energies using various values of A are listed in table 4. The best fit straight line for $(\Delta E_{12})_{TH}$ vs A was determined. Using $(\Delta E_{12})_{EXP}$, it was concluded that Sm, Eu, Gd, and Tb correspond to values of A of 2488, 2408, 2349, and 2251 eV, respectively. The average interval is about 79 eV per rare earth. Extrapolating, then, values for A for all the rare earths were determined and listed in table 5. Also, yttrium is about the same size as erbium (Fontanella et al. 1978b; Shannon 1976) so that A=2014 eV.

One of the advantages of the interface with the 3D picture system is that it is possible to see the reason for the variation of the relative stability of the two complexes. This is shown in figures 3 and 4 where orthographic projection plots of nn and nnn dipoles are shown for an intermediate (A=2300 eV) and a small (A=1600 eV) size trivalent ion in strontium fluoride. Clearly, the substitutional-interstitial interionic distance is smaller for the smaller trivalent for the nnn complex but is actually larger

for the smaller trivalent for the nn complex. This is an example of distortion causing nn complexes to become less stable relative to the nnn complex as the size of the rare earth decreases. That A=1273 eV corresponds to a very small trivalent ion can be seen in figure 5. Other examples of the output of the 3D picture system are given in figures 3 and 4 of the paper by Wintersgill et al. (1980) and figures 3 and 4 of the paper by Andeen et al. (1981).

Following the determination of potentials for various rare earths in strontium fluoride those potentials were used in simulations of calcium fluoride and barium fluoride. The results of the calculations are listed in table 4.

The results for calcium fluoride can be used to comment on a recent controversy concerning the RII relaxation or the B-site of Wright and co-workers (Moore and Wright 1979, 1981; Tallant and Wright 1975; Tallant et al. 1977). It has been shown (Fontanella et al. 1980) that the relaxation data for the RII peak lead to difficulties concerning the relaxation mechanism if it is assigned to a nnn complex. Specifically, equilibrium studies indicate that RII cannot be associated with a nnn→nn jump. That is because the low activation energy (0.15 eV) implies

that the nn and nnn sites should equilibrate quickly at room temperature and thus remain in the same ratio. The experimental data do not support this conclusion. The only alternative is a nnn→nnn reorientation mechanism; however, the very low activation energy (0.15 eV) argues against this conclusion.

The results of the present work support the assertion that RII or the B-site cannot be assigned to a nnn complex. That is because the calculations for a rare earth the size of erbium (A=2014 eV) yield

$$(\Delta E_{12})_{TH} = +0.21 \text{ eV}$$

Consequently, at 100K, about the position of RII, only about 2 in 10^{11} of the ions associated with the simple point defect will be in the nnn position. This conclusion is supported by Baker (1974) who, in his review of the ESR literature implies that the nnn complex has never actually been observed in rare earth doped calcium fluoride using ESR techniques.

It is interesting that RII is only observed for small rare earths (Andeen et al. 1977). This is, of course, the behaviour which might be expected for a nnn complex on the basis of the present calculations though the magnitude of the site populations are not consistent with this identification. However, this same behaviour is observed for RIII which has been

correlated with the D(2a) site of Wright and co-workers (Fontanella et al. 1980; Andeen et al. 1981) and which is some sort of cluster. In fact, it has been suggested (Andeen et al. 1981) that this intimate relationship between RII and RIII may lead ultimately to the identification of these two complexes.

The simulation results for barium fluoride are listed in table 4, and predict that the nn complex will only be stable relative to the nnn complex for the largest rare earths or lanthanum. This is observed experimentally (Laredo et al. 1979, 1980;, Andeen et al. 1981), a low temperature relaxation region being present for lanthanum and cerium (nn) and and a higher temperature relaxation region (nnn) being observed for all of the rare earths. However, the higher temperature relaxation region consists of two closely spaced peaks (Laredo et al. 1980; Andeen et al. 1981). Laredo et al. (1980) have identified one of those as a nn relaxation which they observe for small rare earths. Clearly, the present calculations suggest that this is unlikely as there is no tendency for the nn complex to become stable relative to the nnn complex for small rare earths.

As pointed out previously (Andeen et al. 1981), the conclusion that only nnn complexes exist in barium fluoride doped with small rare earths is supported by

the selective laser excitation work of Miller and Wright (1978a,b) in that they find only one type of simple site in erbium doped barium fluoride.

Clearly, then, a nn→nn reorientation mechanism cannot be responsible for one of the peaks in barium fluoride doped with small rare earths. It is tempting to attribute the two peaks to nnn→nnn and nnn→nn reorientations. However, that cannot be the explanation as both peaks would not be observed via ITC.

A better explanation for one of the two peaks in barium fluoride doped with small rare earths is a cluster. In particular, the position of one of the peaks does depend moderately on the size of the rare earth (Laredo et al. 1980). In fact, the RIV relaxation, which has been observed in both calcium and strontium fluorides (Andeen et al. 1977, 1981) and which has been associated with a "gettered" 2:2:2 (Wintersgill et al. 1980; Andeen et al. 1981), depends strongly upon the nature of the rare earth. However, the experimental data concerning the barium fluoride relaxations to date (Laredo et al. 1980; Andeen et al. 1981) do not support assigning either to a cluster. Further work is necessary for their identification.

4.2.2. Effect of Pressure on Reorientation Enthalpies

As a second test of the simulation program, the reorientation enthalpy was calculated for jumps of an interstitial between nearest neighbour equivalent sites via the interstitialcy mechanism for calcium fluoride and strontium fluoride. In the present calculations, the saddle point of the migrating ion was not predetermined. Only one coordinate of the diffusing ion was fixed. The saddle point was then determined by minimization at successive values of a single coordinate of the diffusing ion. The activation enthalpy was then taken to be the maximum value of the lattice energy along the path of the diffusing ion. The results are listed in table 6 together with the corresponding experimental values. The theoretical values are about 0.1-0.2 eV higher than the experimental values. While it is tempting to assign the discrepancy to the rare earth potential, the difference may be more fundamental in that there is no reason to expect a static calculation to accurately simulate an inherently dynamical process. However, the calculations do show only a small decrease in the enthalpy as the size of the rare earth decreases. That is in agreement with experiment.

Next, the effect of pressure on the reorientation enthalpy for nn→nn jumps in strontium fluoride doped with a large rare earth was determined

theoretically from

$$\left(\frac{\partial E}{\partial P}\right)_{TH} = -\chi_T V\left(\frac{\partial E}{\partial V}\right) \qquad (10)$$

where χ_T is the isothermal compressibility for strontium fluoride. The enthalpy was found to increase by about 0.0042 eV when the lattice constant was decreased by about 0.05% (0.1 GPa pressure). Thus,

$$\left(\frac{\partial E}{\partial P}\right)_{TH} = 42 \text{ meV/GPa}$$

which is in excellent agreement with the experimental value of 41 meV/GPa (Fontanella et al. 1981). (In the present calculation, the central region was not further relaxed upon application of pressure, only the lattice constant was changed.) The agreement is better than expected considering the uncertainty in the experiment and the nature of the theoretical calculation.

In summary, while the program does not yield good values of reorientation enthalpies, the effects of small perturbations, such as pressure or small shifts in ion size, on the enthalpy are reproduced quite well.

5. Conclusions

In summary, then, the results of a new computer program for modeling ionic solids and best-fitting data are presented. The techniques are applied to the

problem of simple point defects in rare earth doped alkaline earth fluorides. A combination of the techniques has led to the following results:

1. Potentials are obtained for all the rare earths, lanthanum, and yttrium. Those were obtained by a combination of theoretical and experimental results for rare earths in strontium fluoride.
2. Calculations for rare earths in calcium fluoride clearly show that the nnn complex should not be observable in the vicinity of room temperature or below except for possibly the smallest rare earths and thus rule out assigning the RII relaxation or the B site to a nnn complex.
3. Calculations for barium fluoride clearly show that the nn complex should only be observable for the largest rare earths or lanthanum and thus rule out nn→nn reorientations for small rare earths.
4. Calculated nn→nn reorientation enthalpies for calcium fluoride and strontium fluoride are found to be larger than the experimental values, however, the variation of the enthalpy with the size of the rare earth and with pressure agree reasonably well with experiment.

Acknowledgments

This work was supported in part by the Naval

Academy Research Council and the Office of Naval Research.

References

Andeen C, Schuele D, and Fontanella J 1972 Phys. Rev. B6 591-5

Andeen C G, Fontanella J J, Wintersgill M C, Welcher P J, Kimble R J Jr., and Matthews G E Jr., 1981 J. Phys C: Solid St. Phys., 14 3557-74

Andeen C, Link D J and Fontanella J J 1977 Phys. Rev. B16 3762-67

Baker J M 1974 in Crystals with the Fluorite Structure ed. W. Hayes, Clarendon Press, Oxford.

Catlow C R A, 1976 J. Phys C: Solid St. Phys. 9 1845-69

Catlow C R A, Norgett M J and Ross T A 1977 J Phys C: Solid St. Phys. 10 1627-40

Edgar A and Welsh H K 1979 J. Phys. C:Solid St. Phys. 12 703-13

Fontanella J, Andeen C A, and Schuele D 1972 Phys. Rev. B6 582-90

Fontanella J, Jones D L, and Andeen C, 1978a Phys. Rev.

B18 4454-61

Fontanella J, Andeen C, and Schuele D 1978b Phys. Rev. B18 3429-31

Fontanella J J, Treacy D J and Andeen C 1980 J. Chem Phys. 72 2235-44

Fontanella J J, Wintersgill M C, Chadwick A V, Saghafian R, and Andeen C G, 1981 J. Phys C: Solid St. Phys 14 2451-64

Gibbs D F and Jarman M 1962 Phil. Mag. 7 663-70.

Laredo E, Puma M, and Figueroa D R 1979 Phys. Rev. B19 2224-30

Laredo E, Figueroa D R, and Puma 1980 J. de Physique 41 C6-451-4

Matthews G E Jr and Crawford J H Jr 1977 Phys. Rev. B15 55-60

Miller M P and Wright J C 1978a J. Chem. Phys. 68 1548-62

Miller M P and Wright J C 1978b Phys. Rev. B18 3753-6

Moore D S and Wright J C 1981 J. Chem. Phys. 74 1626-36.

Moore D S and Wright J C 1979 Chem. Phys. Letters 66 173-6

Mott N F and Littleton M J 1938 Trans. Far. Soc. 34 485-99.

Rheinboldt W G 1974 Methods for Solving Systems of Nonlinear equations, Society for Industrial and Applied Mathematics, Philadelphia

Shannon R D 1976 Acta Cryst. A32 751-67

Tallant D R, Moore D S and Wright J C 1977 J. Chem. Phys. 67 2897-2907

Tallant D R and Wright J C 1975 J. Chem. Phys. 63 2074-85

Wintersgill M C, Fontanella J J, Welcher P, Kimble R J Jr., and Andeen C G 1980 J. Phys. C: Solid State Phys. 13 L661-6

Table 1. Values of the logarithmic derivative of the polarizability determined using the data of Andeen et al. (1972) and Fontanella et al. (1972).

	$\frac{V}{\alpha}\left(\frac{\partial\alpha}{\partial V}\right)_T$
CaF_2	2.09
SrF_2	2.03
BaF_2	1.92
LiF	2.01
NaF	2.32
NaCl	2.12
NaBr	2.05
KCl	2.05
KBr	2.00

Table 2. Polarizabilities of ions in the alkaline earth fluorides in units of 10^{-40}N/Coul^2-m. The values include both electronic and ionic effects.

	α_F	α_{AE}
Ca	1.96	5.02
Sr	1.66	6.54
Ba	1.39	9.17

Table 7. Activation parameters for rare earth doped strontium fluoride.

RE	C_1 (K)	E_{21} eV	$(\tau_o)_1$ 10^{-14}s	α_1	C_2 (K)	E_{21} eV	$(\tau_o)_2$ 10^{-14}s	α_2	ΔS_{12} k	ΔE_{12} eV	RMS error (10^{-5})
La	40.5	0.483	1.48	0.031							64
Ce	39.3	0.471	1.58	0.037							90
Pr	62.4	0.474	1.63	0.039							103
Nd	71.5	0.483	0.985	0.06							271
Sm	54.1	0.445	3.80	0.04	538.6	0.626	2.38	.135	.736	.111	56.5
Eu	38.6	0.457	2.60	0.026	349.6	0.638	1.95	.064	.598	.080	45.7
Gd	61.1	0.461	2.50	0.034	451.3	0.652	1.39	.066	.75	0.0575	112.7
Tb	42.7	0.447	3.34	0.051	436.6	0.0657	1.08	.037	.133	0.020	84.5
Dy					215.5	0.682	0.56	0.040			165
Ho					273	0.683	0.62	0.035			349
Y					274	0.697	0.38	0.046			257
Er					295	0.698	0.32	0.037			332
Tm					265	0.683	0.34	0.042			224
Yb					256	0.683	0.28	0.046			173

Table 4. Results of the computer simulation for $(\Delta E_{12})_{TH}$

A(eV)	$(\Delta E_{12})_{TH}$(eV)		
	CaF_2	SrF_2	BaF_2
2700	+0.55	+0.19	-0.022
2600	+0.50	+0.16	-0.057
2400	+0.41	+0.079	-0.128
2200	+0.31	-0.002	-0.20
2000	+0.20	-0.08	-0.26
1800	+0.09	-0.15	-0.29

Table 5. Values of A in the rare earth potential $V(r) = A \exp(-r/0.2997\text{Å})$. The values with the asterisks were determined by comparing $(\Delta E_{12})_{TH}$ and $(\Delta E_{12})_{EXP}$ and the remainder by extrapolation.

Rare earth	A(eV)	Rare earth	A(eV)
La	2883	Tb	2251*
Ce	2804	Dy	2172
Pr	2725	Ho	2093
Nd	2646	Er(Y)	2014
Sm	2488*	Tm	1935
Eu	2408*	Yb	1856
Gd	2349*	Lu	1777

Table 6. Reorientation enthalpies for nn→nn jumps of an interstitial via the interstitialcy mechanism.

A(eV)	Theory	Experiment
CaF_2		
2600 (~Nd)	0.69	0.43[a]
2400 (~Eu)	0.67	0.414[a]
2000 (~Er)	0.61	0.406[a]
SrF_2		
2600 (~Nd)	0.564	0.48[b]
2400 (~Eu)	0.562	0.46[b]

---

a. Andeen et al. (1977).

b. From table 3.

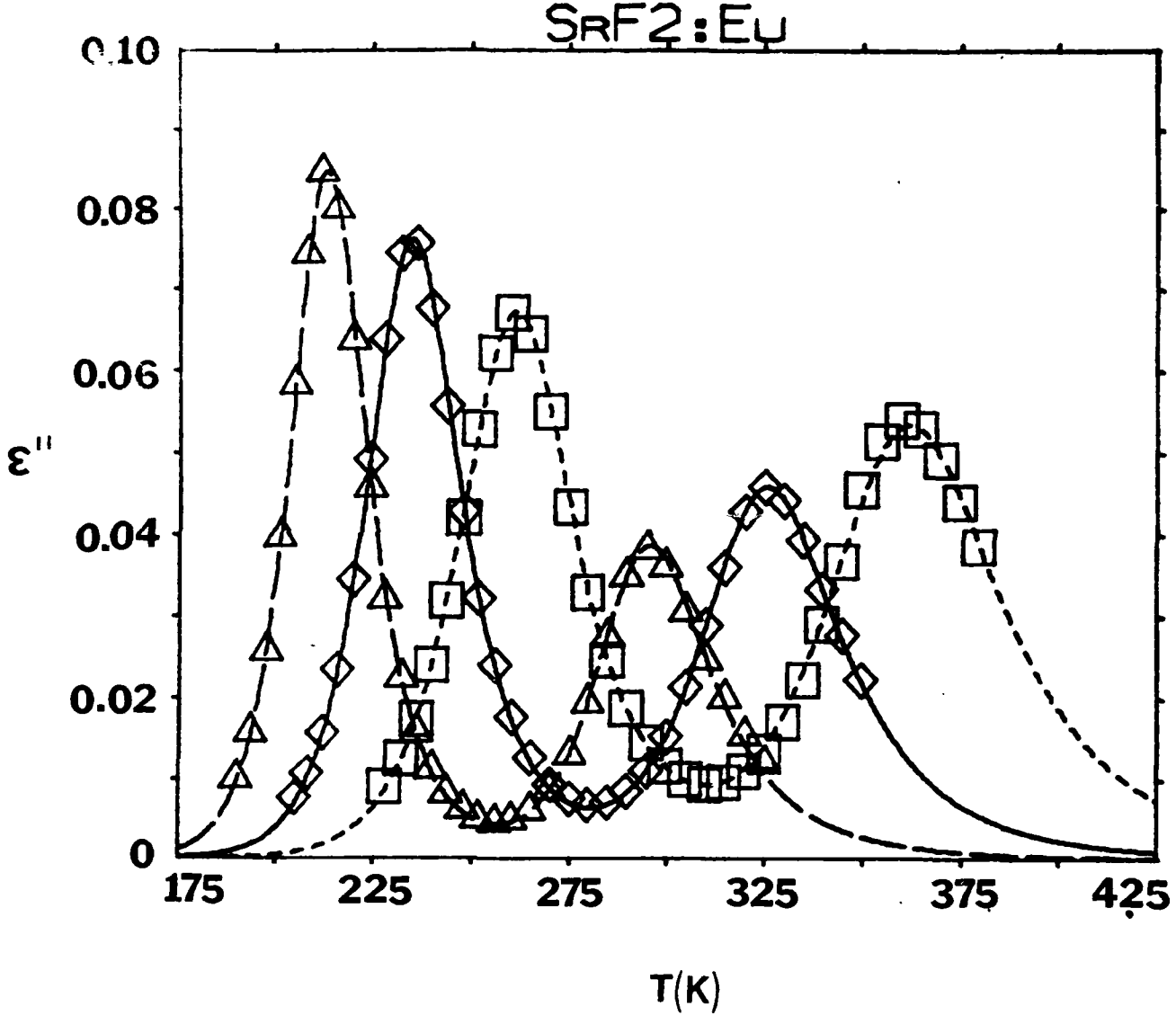

Figure 1. ε" vs absolute temperature for europium doped strontium fluoride. △ 100 Hz data; ◇ 1000 Hz data; □ 10000 Hz data; Best-fit curves.

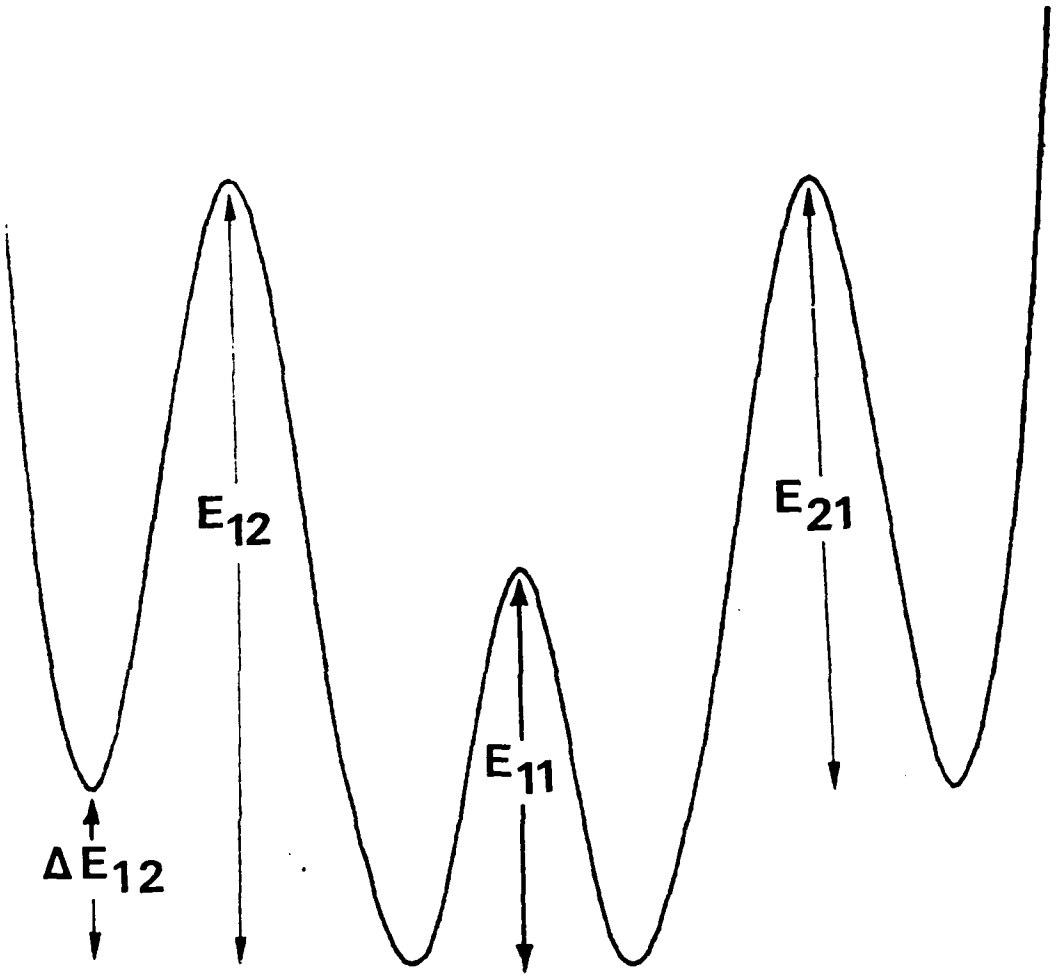

Figure 2. Potential wells for nn and nnn dipoles in the alkaline earth fluorides.

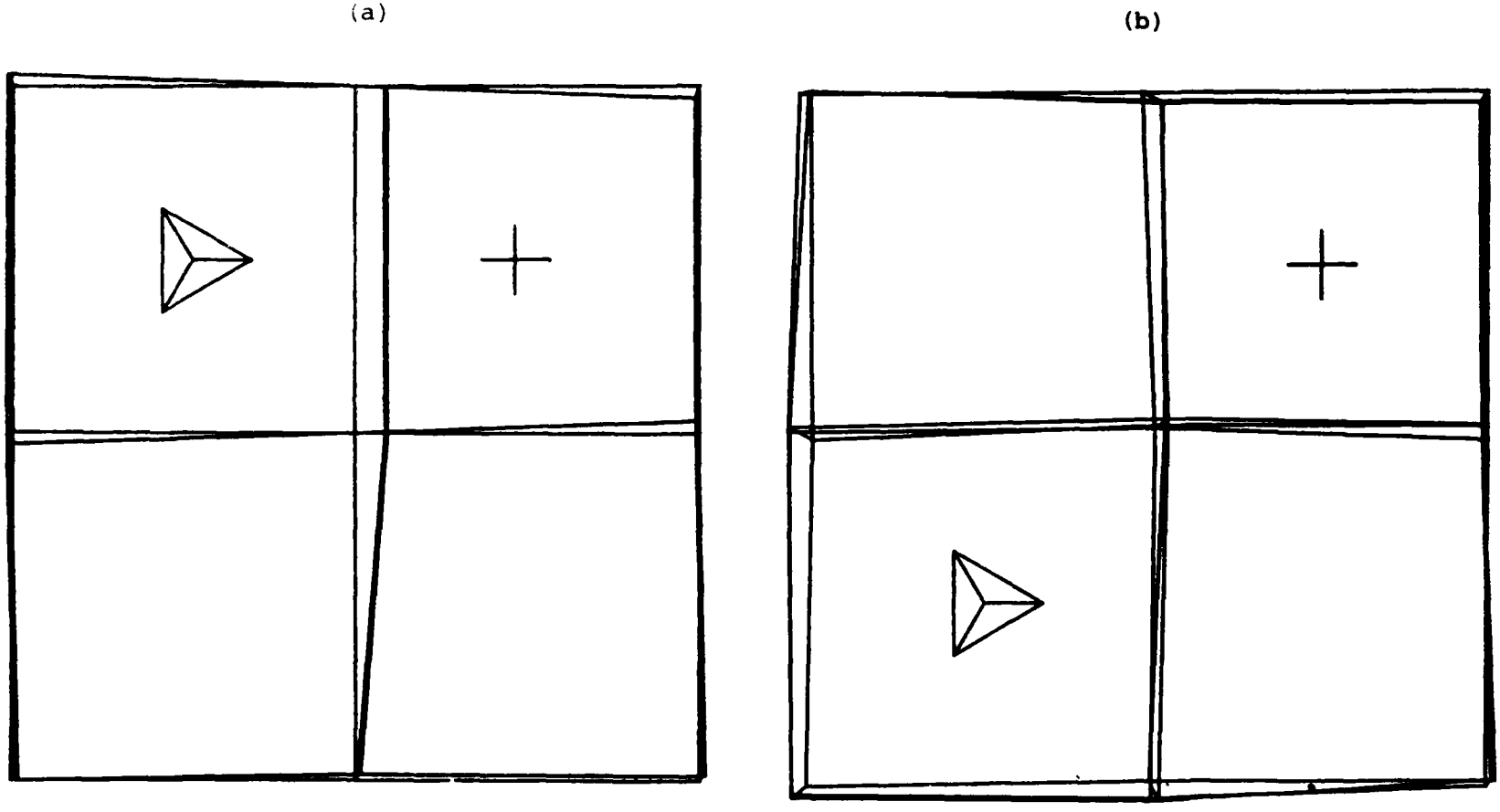

Figure 3. Orthographic projection along the (100) direction for an intermediate size rare earth in strontium fluoride (A=2300 eV). The plus indicates the position of the rare earth and the tetrahedron represents the charge compensating interstitial fluorine. The straight lines connect lattice fluorines. (a) nn complex (b) nnn complex.

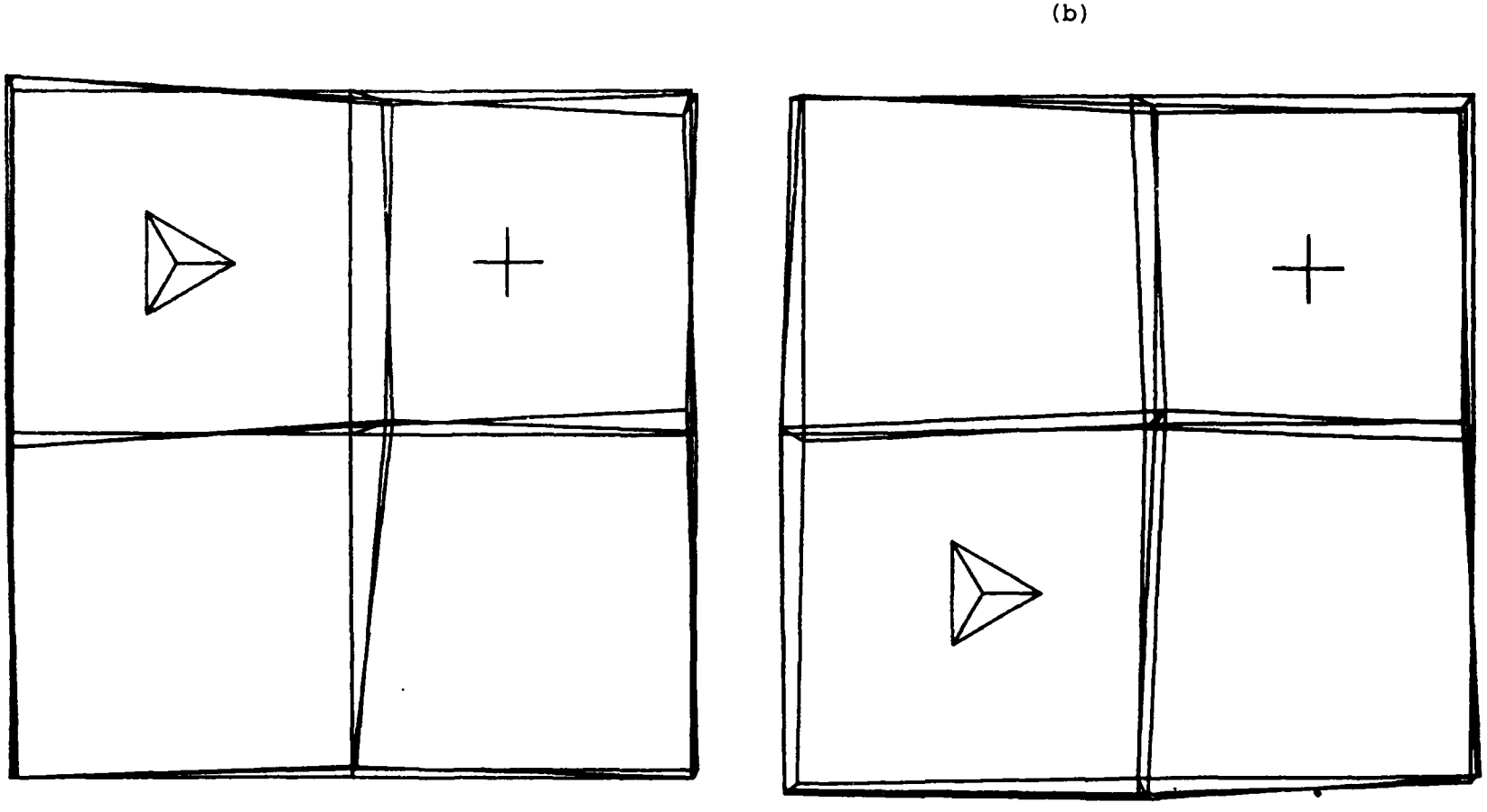

Figure 4. Orthographic projection along the (100) direction for a small trivalent ion in strontium fluoride (A=1600 eV). The designations are the same as those for Figure 3.

(a)

(b)

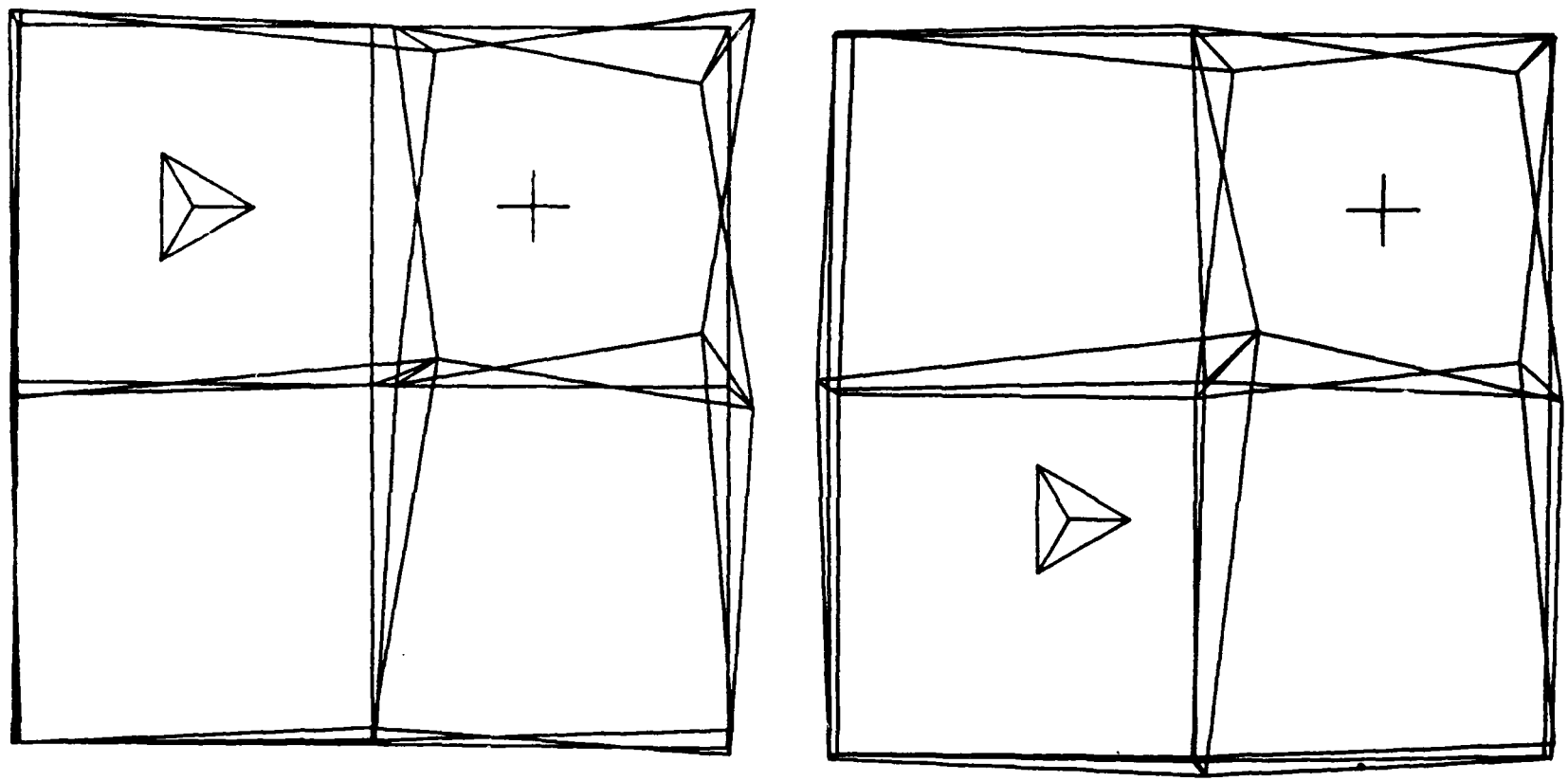

Figure 5. Orthographic projection along the (100) direction for a very small trivalent ion in strontium fluoride (A=1273 eV). The designations are the same as those for figure 3.

Appendix A. The Minimization Philosophy.

The minimization strategy is the same in both our parameter fitting of data and in the computer modeling programs. While the basic idea is well known, its implementation in this application is not.

In order to develop the notation, let us first consider the question of finding a solution to the vector equation:

$$\underset{\sim}{g}(\underset{\sim}{a}) = 0$$

where $\underset{\sim}{a} = \{a_1, a_2, \ldots a_p\}$,

and

$$\underset{\sim}{g}(\underset{\sim}{a}) = \{g_1(\underset{\sim}{a}), g_2(\underset{\sim}{a}), \ldots, g_p(\underset{\sim}{a})\}.$$

Thus, we are trying to find a simultaneous solution to the p nonlinear equations:

$$g_i(a_1, a_2, \ldots, a_p) = 0.$$

Suppose we refer to such a solution as

$$\underset{\sim}{a}^* = \{a_1^*, a_2^*, \ldots, a_p^*\}$$

and we are given a vector, $\underset{\sim}{a}$, which is close to our solution, $\underset{\sim}{a}^*$. Then in order to find our solution, we have just to find

$$\Delta\underset{\sim}{a} = \underset{\sim}{a}^* - \underset{\sim}{a} \quad \text{or} \quad \Delta a_i = a_i^* - a_i .$$

If $\Delta\underset{\sim}{a}$ is sufficiently small, then vector calculus assures us of the approximation

$$g_j(\underset{\sim}{a}+\Delta\underset{\sim}{a}) \approx g_j(\underset{\sim}{a}) + \sum_{i=1}^{p} \frac{\partial g_j}{\partial a_i} \Delta a_i$$

$$= g_j(\underset{\sim}{a}) + (\underset{\sim}{\nabla} g_j) \cdot (\Delta\underset{\sim}{a}),$$

where

$$\underset{\sim}{\nabla} g_j = \{\frac{\partial g_j}{\partial a_1}, \ldots, \frac{\partial g_j}{\partial a_p}\}$$

The above equations can be summarized by the equation:

$$\underset{\sim}{g}(\underset{\sim}{a}+\Delta\underset{\sim}{a}) \approx \underset{\sim}{g}(\underset{\sim}{a}) + (\underset{\sim}{J}_{\underset{\sim}{g}})(\Delta\underset{\sim}{a}) \qquad (1)$$

where $\underset{\sim}{J}_{\underset{\sim}{g}}$ is the p by p Jacobian matrix given by:

$$\underset{\sim}{J}_{\underset{\sim}{g}} = \left(\frac{\partial g_j}{\partial a_i}\right).$$

Of course, we want $\Delta\underset{\sim}{a}$ to satisfy $\underset{\sim}{g}(\underset{\sim}{a}+\Delta\underset{\sim}{a})=0$. Thus, we use equation (1) to solve for $\Delta\underset{\sim}{a}$:

$$\Delta\underset{\sim}{a} = -(\underset{\sim}{J}_{\underset{\sim}{g}})^{-1}(\underset{\sim}{g}(\underset{\sim}{a})). \qquad (2)$$

The technique for finding $\underset{\sim}{a}^*$ then amounts to finding a close initial value, say $\overset{a}{\sim}_o$, and then iterating by the formula

$$\underset{\sim}{a}_{n+1} = \underset{\sim}{a}_n - (\underset{\sim}{J}_{\underset{\sim}{g}})^{-1}(\underset{\sim}{g}(\underset{\sim}{a}_n)) \qquad (3)$$

where the Jacobian is evaluated at $\overset{a}{\sim}_n$. If $\overset{a}{\sim}_o$ is "sufficiently close," then the sequence

$$\underset{\sim}{a}_o, \underset{\sim}{a}_1, \cdots \underset{\sim}{a}_n, \cdots$$

will converge fairly rapidly to the solution, $\underset{\sim}{a}^*$. This is of course the Newton-Raphson iterative method for finding a minimum. In the computer model, we let S represent the total energy of the ions. For data fitting, S is the sum of the squares of the differences between the data and fitted values.

Appendix B. Curve Fitting.

For data fitting, we are given data values:

$$(x_i, y_i)$$

and the equation to be fitted:

$$y = f(x,\underset{\sim}{a})$$

where $\underset{\sim}{a}$ represents the set of parameters to be fit. A solution is merely a value, $\underset{\sim}{a}^*$, that minimizes the value of the function:

$$S = \sum_{i=1}^{N} |y_i - f(x_i,\underset{\sim}{a})|^2 \qquad (4)$$

where N is the number of data points. In this case, we are attempting to find a solution to the vector equation:

$$\underset{\sim}{\nabla}S = \{\frac{\partial S}{\partial a_1},\frac{\partial S}{\partial a_2},\ldots,\frac{\partial S}{\partial a_p}\} = 0$$

Given a starting value, $\underset{\sim}{a}_o$, we then iterate using the appropriate modification of equation (3):

$$\underset{\sim}{a}_{n+1} = \underset{\sim}{a}_n - (\underset{\sim}{H})^{-1}(\underset{\sim}{\nabla}S) \qquad (5)$$

where $\underset{\sim}{H}$ is the Hessian (matrix of second partials) of S; i.e.

$$\underset{\sim}{H} = \left(\frac{\partial^2 S}{\partial a_i \partial a_j}\right)$$

and $\underset{\sim}{\nabla}S$ is the gradient, both evaluated at $\underset{\sim}{a}_n$.

For our curve-fitting, we have developed software using APL on the local timesharing system, NATS (Naval Academy Time-Sharing System), which is based on the DTSS (Dartmouth Time Sharing System). We

chose APL for the following reasons:

1. APL is an interpreter and therefore lends itself well to interactive programming.

2. APL has a wide range of built-in functions including virtually all of the so-called scientific functions.

3. Our implementation of APL has excellent built-in graphics capabilities.

The APL package we have developed has routines for data input, least squares fitting and graphics display of the data along with the theoretical curve given by the current values of the fitted parameters.

Some details about the least squares routine are now in order. One of the functions included in the package is a function S that depends only on the parameters a_1 through a_p using equation (4). Thus, S is the sum of the squares of the differences between the measured value, y_i, and the theoretical value, $f(\underset{\sim}{x}_i, \underset{\sim}{a})$ at each data point, $\underset{\sim}{x}_i$. We use the vector notation for $\underset{\sim}{x}_i$ because there is no necessity for the data points to be scalars. In fact, in this paper, the $\underset{\sim}{x}_i$ are the frequencies and the temperature and y_i is the corresponding measured imaginary dielectric constant. In order to use Newton's formula, we must then calculate $\underset{\sim}{\nabla S}$ and $\underset{\sim}{H}$. The appropriate partial derivatives are calculated numerically by the following

formulae:

$$\frac{\partial S}{\partial a_i} \approx \frac{S(\underset{\sim}{a}+\delta\underset{\sim}{a}_i) - S(\underset{\sim}{a}-\delta\underset{\sim}{a}_i)}{2\delta}$$

and

$$\frac{\partial^2 S}{\partial a_i \partial a_j} \approx \left(\frac{1}{4\,\delta^2}\right) \{S(\underset{\sim}{a}+\delta\underset{\sim}{a}_i+\delta\underset{\sim}{a}_j) - S(\underset{\sim}{a}+\delta\underset{\sim}{a}_i-\delta\underset{\sim}{a}_j) - S(\underset{\sim}{a}-\delta\underset{\sim}{a}_i+\delta\underset{\sim}{a}_j) + S(\underset{\sim}{a}-\delta\underset{\sim}{a}_i-\delta\underset{\sim}{a}_j)\}$$

where $\delta\underset{\sim}{a}_i$ is a vector with δ in the ith position and zero elsewhere. The starting values for $\underset{\sim}{a}$ are supplied by the user. Also, the user supplies the $\delta\underset{\sim}{a}_i$, which are the sensitivity values by which the parameters are varied in the calculation of the partial derivatives. These sensitivity values are based on the user's experience and are often varied as the fit improves. In addition to this, parameters are sometimes "transformed" in order to make them more amenable to analysis. A case in point is τ_o, the reciprocal frequency factor. Rather than fit a parameter that can easily vary by a few orders of magnitude, it is much better to fit $\ln(\tau_o)$ and then determine τ_o by exponentiation.

After determining sensitivities, the user then commands the computer to begin the least squares fit.

At the start of the routine, the computer calculates and stores $S(\underset{\sim}{a})$ as well as the current parameter values. In the process of calculating $\underset{\sim}{\nabla} S$ and $\underset{\sim}{H}$, it evaluates S in the vicinity of $\underset{\sim}{a}$, using standard difference quotient approximations for the derivatives. If one of these values happens to be at the current minimum value for S, both it and the corresponding parameter values are stored. Finally, $\underset{\sim}{\nabla} S$ and $\underset{\sim}{H}$ are used to obtain:

$$\Delta \underset{\sim}{a} = -(\underset{\sim}{H})^{-1}(\underset{\sim}{\nabla} S) \quad .$$

The values for

$$S(\underset{\sim}{a}+\Delta \underset{\sim}{a}) \qquad \text{and} \qquad S(\underset{\sim}{a}+2\Delta \underset{\sim}{a})$$

are then computed. A parabolic fit is applied to the values

$$S(\underset{\sim}{a}+c\Delta \underset{\sim}{a}) \qquad (c = 0,1,2)$$

to estimate the value c* for which

$$S(\underset{\sim}{a}+c^*\Delta \underset{\sim}{a})$$

is a minimum. Finally,

$$S(\underset{\sim}{a}+c^*\Delta \underset{\sim}{a})$$

is evaluated. At this point the routine chooses the point, $\underset{\sim}{a}^*$, for which the computed value of S was

smallest, and alters the current parameter values accordingly. Iterations are continued until no further significant progress is made.

There are several valuable features to the routine that greatly enhance the purely numerical techniques of minimization. The particular numerical algorithm chosen for doing the minimization provides a nice balance between the sure, but slowly converging, grid search method, and the rapidly converging, but somewhat unstable Newton method. As mentioned in the introduction, the parabolic fit essentially recovers the curvature in the Newton-Raphson (gradient) direction and thus describes to some extent the metric on the graph of the squared difference sum function or the energy function.

Finally, and by far the most important feature of all, is the interactive nature of the numerical techniques and graphic display of the fit in its current state. The ability of the individual to interpret and evaluate graphical data is far superior to any known purely numeric computer algorithm. At times, especially when the numerical methods fail to improve the fit when obvious improvements can be made, the experienced user can manually adjust parameter values and sensitivity values in an attempt to get the parameters into a region where the numerical methods

will once again converge. This interaction has proved to be the most valuable feature of all.

This interactive aspect is of course not available with the defect simulation package, but experimentation has established that the above minimization procedure nonetheless leads to rapid convergence of ion location. The instability where one ion converges to another's location (due to the two getting too close) can be easily dealt with by giving the ions an arbitrarily large repulsive potential within an appropriate radius. Statistics kept during all runs to date show that both the grid search and parabolic fit in the Newton direction are techniques well worth inclusion in the defect simulation package. Specifically, inclusion of the parabolic fit feature appears to have sped up convergence by a factor of ten. This makes the running time requirements quite acceptable.

Appendix C. Defect Simulations.

We now give more details of the operation of the defect simulation package. The model contains about 150 movable ions (5x5x5 fluorines plus appropriate cations). These are "surrounded" by a continuum of fixed ions each of which is assigned a total (electronic and ionic) polarizability. The

electrostatic calculations for a given ion in the central region are performed exactly for the surrounding cube of 11x11x11 fluorines plus cations and the remaining electrostatic energy is approximated via a Madelung sum.

One or more defect ions can be added to a file containing the basic model including substitutionals, interstitials, or vacancies. The lattice is then allowed to relax to the minimum energy configuration. That is, for each ion in turn an approximate energy gradient is evaluated, representing the net force on that ion due to the other ions in the model. The ion is allowed to move an appropriate amount in the direction specified by the force (gradient), and then the computer moves on to the next ion. All this is done a large number of times (1000 to 5000 moves being necessary) . The energy function used will be discussed in the next section.

One crucial factor is the question of how far each ion is to move. This should depend on the force exerted on that ion but should not be too great, as the ions in actuality all move simultaneously. One does not wish to reach a physically implausible configuration by moving one ion around excessively.

We proceed by starting with initial values based on experience and trial-and error experimentation with

the model. Starting with a Newton-Raphson approach loosely controlled, reasonable values for the move are established, and these are what are initially used. Subsequently, each ion is allowed to move only as far as it moved the previous time; half as far in most cases (down to a minimum size allowed move). Ions with largest potential move are moved first. This helps speed up the convergence process.

Having dealt with the question of how far to move, the next question is in which direction each ion is to be moved. For each ion, the following information is stored: reference coordinates, type, shell coordinates, nucleus coordinates, and move size. The shell is specified by a given radius (ion size) and is assumed to be roughly spherical. Its coordinates are those of its center, which should be roughly the same as the nucleus coordinates. Move size is the size of the largest distance the shell center and nucleus are allowed to move.

The program calculates the energy

$$G(x_1,\ldots,x_6)$$

stemming from the ion under consideration being at shell location (x_1, x_2, x_3) and nucleus position (x_4, x_5, x_6). The force on the ion is $-\nabla G$ which is approximated using the first difference,

$$\frac{\partial G}{\partial x_1} \approx \frac{G(x_1+\delta, x_2, \ldots, x_6) - G(x_1-\delta, x_2, \ldots, x_6)}{\delta}$$

As only the direction is needed, the division by the step size δ to give the difference quotient is not performed, to save time. A standard Newton-Raphson routine to locate a zero of the force function $-\nabla G$ is performed. Thus the force on the ion is estimated to be zero when the ion at location $\underset{\sim}{x}$ is moved to the new location given by $\underset{\sim}{x} + \Delta\underset{\sim}{x}$, where $\Delta\underset{\sim}{x}$ is given by

$$\Delta\underset{\sim}{x} = -(\underset{\sim}{H})^{-1}(\underset{\sim}{\nabla}G)$$

Here $\underset{\sim}{H}$ is the Hessian matrix of second derivatives of G or equivalently the matrix of partials of the force $F = -\underset{\sim}{\nabla}G$. See section 2 above.

The second partials in H are estimated as second differences. Note that we thus take

$$\Delta\underset{\sim}{x} \approx -(\underset{\sim}{H})^{-1}(\underset{\sim}{\nabla}G)\,\delta$$

where $\underset{\sim}{H}$ is the approximate Hessian and ∇G the approximate gradient. In all these difference quotients, division by the step size δ can be completely eliminated, thus avoiding unnecessary expensive machine divisions. A further benefit is the increased numerical stability experienced in the inversion of the matrix H.

The Newton-Raphson technique notoriously suffers from poor efficiency when near the zero, i.e. when the ion is nearly in a minimal energy position. This is

also true near local minima or saddle points of the energy function. Thus it has proved useful to test the energy at the points being used in the partial derivative approximations, i.e. conduct a "grid search", as the energy has to be calculated anyway for the partials.

Thus if the energy is lower at one of the locations used in the partial derivative calculations than at the Newton-Raphson site, the former is chosen as the new ion location. A further refinement is possible. It is plausible that near the local minimum of the energy function (much as with a least squares function) that the geometry is "parabolic", i.e. one anticipates that along any line through the current location of the ion the energy function's graph will be parabolic. A parabolic fit in the Newton-Raphson direction is performed, as described in section ? above. That most moves are being made in this fashion is not too surprising, as the parabolic fit is essentially equivalent to finding the curvature at the Newton-Raphson site in the direction of the gradient.

For maximum efficiency, the method of approximating partial derivatives is not quite as described above. First, note that the matrix of second partials of the energy function G for a given ion may be reasonably assumed to be symmetric. Theoretically

this is justified as we are working with a matrix of second partials, and continuity is not a drastic assumption.

The shell and nucleus in the standard shell model are joined by springs, i.e. our matrix H of second partials is of the form

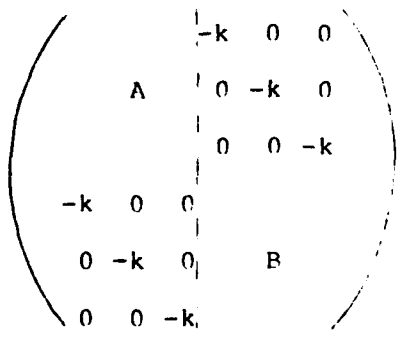

Here k is the spring constant, A is the dependence of the energy on the shell position, and B is the portion due to the nucleus.

We return to the question of approximating the remaining second partials of the energy function. So as to combine a grid search with a Newton-Raphson technique, we should estimate the partial , for example, as the difference quotient

$$\frac{\partial G}{\partial x_1} \approx \frac{G(x_1+\delta, x_2, \ldots, x_6) - G(x_1-\delta, x_2, \ldots, x_6)}{2\delta}$$

Similarly, the second partial should be estimated as

$$\frac{\partial^2 G}{\partial x_1 \partial x_2} \approx \frac{1}{4\delta^2} \{G(x_1+\delta, x_2+\delta, \ldots, x_6) - G(x_1+\delta, x_2-\delta, \ldots, x_6)$$

$$- G(x_1-\delta, x_2+\delta, \ldots, x_6) + G(x_1-\delta, x_2-\delta, \ldots, x_6)\}$$

Initially δ differed for each coordinate but it was found to be simpler to use the same δ in each coordinate.

However, this means that we must evaluate the energy at 18 points. If one thinks of the ion under study as being at the center of a cube of side 2δ, we are evaluating at the center of each face and edge of the cube. Instead, the program evaluates the energy at the 8 points corresponding to the corners of the cube (i.e. all of the 3 shell/nucleus coordinates varied by either $\pm\delta$, rather than just one or two being simultaneously changed). The value at the middle of an edge is approximated as the average of the two corner values, for the corners on the ends of that edge. The value of the energy function at the middle of a face of the cube is approximated as the average of the values at the four corners of that face. Thus at the price of a little added complexity, the evaluations of the energy function and hence the time demands of the program may be halved.

Note that the previous move size δ is the same

as the δ used in these difference quotients.

Other refinements are: (i) the move size δ is stored as $\geq .001$ unless a (smaller) Newton-Raphson move has been made. (ii) if the Hessian is not stably invertible, only a "grid search" is performed. (iii) no division by δ or by δ^2 is performed.

472:GAN:716-4
94/GEN

TECHNICAL REPORT DISTRIBUTION LIST, GEN

	No. Copies
Office of Naval Research Attn: Code 413 800 North Quincy Street Arlington, Virginia 22217	2
ONR Pasadena Detachment Attn: Dr. R. J. Marcus 1030 East Green Street Pasadena, California 91106	1
Commander, Naval Air Systems Command Attn: Code 310C (H. Rosenwasser) Department of the Navy Washington, D.C. 20360	1
Defense Technical Information Center Building 5, Cameron Station Alexandria, Virginia 22314	12
Dr. Fred Saalfeld Chemistry Division, Code 6100 Naval Research Laboratory Washington, D.C. 20375	1
U.S. Army Research Office Attn: CRD-AA-IP P. O. Box 12211 Research Triangle Park, N.C. 27709	1
Mr. Vincent Schaper DTNSRDC Code 2803 Annapolis, Maryland 21402	1
Naval Ocean Systems Center Attn: Dr. J. Yamamoto Marine Sciences Division San Diego, California 91232	1
Naval Ocean Systems Center Attn: Mr. Joe McCartney San Diego, California 92152	1
Naval Weapons Center Attn: Dr. A. B. Amster, Chemistry Division China Lake, California 93555	1
Naval Civil Engineering Laboratory Attn: Dr. R. W. Drisko Port Hueneme, California 93401	1
Dean William Tolles Naval Postgraduate School Monterey, California 93940	1
Scientific Advisor Commandant of the Marine Corps (Code RD-1) Washington, D.C. 20380	1
Naval Ship Research and Development Center Attn: Dr. G. Bosmajian, Applied Chemistry Division Annapolis, Maryland 21401	1
Mr. John Boyle Materials Branch Naval Ship Engineering Center Philadelphia, Pennsylvania 19112	1
Mr. A. M. Anzalone Administrative Librarian PLASTEC/ARRADCOM Bldg 3401 Dover, New Jersey 07801	1

TECHNICAL REPORT DISTRIBUTION LIST, 359

	No. Copies
Dr. Paul Delahay Department of Chemistry New York University New York, New York 10003	1
Dr. E. Yeager Department of Chemistry Case Western Reserve University Cleveland, Ohio 41106	1
Dr. D. N. Bennion Department of Chemical Engineering Brigham Young University Provo, Utah 84602	1
Dr. R. A. Marcus Department of Chemistry California Institute of Technology Pasadena, California 91125	1
Dr. J. J. Auborn Bell Laboratories Murray Hill, New Jersey 07974	1
Dr. Adam Heller Bell Laboratories Murray Hill, New Jersey 07974	1
Dr. T. Katan Lockheed Missiles and Space Co., Inc. P. O. Box 504 Sunnyvale, California 94088	1
Dr. Joseph Singer, Code 302-1 NASA-Lewis 21000 Brookpark Road Cleveland, Ohio 44135	1
Dr. B. Brummer EIC Incorporated 55 Chapel Street Newton, Massachusetts 02158	1
Library P. R. Mallory and Company, Inc. Northwest Industrial Park Burlington, Massachusetts 01803	1
Dr. P. J. Hendra Department of Chemistry University of Southampton Southampton S00 5NH United Kingdom	1
Dr. Sam Perone Chemistry & Materials Science Department Laurence Livermore National Lab. Livermore, California 94550	1
Dr. Royce W. Murray Department of Chemistry University of North Carolina Chapel Hill, North Carolina 27514	1
Naval Ocean Systems Center Attn: Technical Library San Diego, California 92152	1
Dr. C. E. Mueller The Electrochemistry Branch Materials Division, Research and Technology Department Naval Surface Weapons Center White Oak Laboratory Silver Spring, Maryland 20910	1
Dr. G. Goodman Johnson Controls 5757 North Green Bay Avenue Milwaukee, Wisconsin 53201	1
Dr. J. Boechler Electrochimica Corporation Attn: Technical Library 2485 Charleston Road Mountain View, California 94040	1
Dr. P. P. Schmidt Department of Chemistry Oakland University Rochester, Michigan 48063	1

TECHNICAL REPORT DISTRIBUTION LIST, 359

	No. Copies
Dr. H. Richtol Chemistry Department Rensselaer Polytechnic Institute Troy, New York 12181	1
Dr. A. B. Ellis Chemistry Department University of Wisconsin Madison, Wisconsin 53706	1
Dr. M. Wrighton Chemistry Department Massachusetts Institute of Technology Cambridge, Massachusetts 02139	
Larry E. Plew Naval Weapons Support Center Code 30736, Building 2906 Crane, Indiana 47522	1
S. Ruby DOE (STOR) 600 E Street Providence, Rhode Island 02192	1
Dr. Aaron Wold Brown University Department of Chemistry Providence, Rhode Island 02192	1
Dr. R. C. Chudacek McGraw-Edison Company Edison Battery Division Post Office Box 28 Bloomfield, New Jersey 07003	1
Dr. A. J. Bard University of Texas Department of Chemistry Austin, Texas 78712	1
Dr. M. M. Nicholson Electronics Research Center Rockwell International 3370 Miralema Avenue Anaheim, California	1
Dr. R. P. Van Duyne Department of Chemistry Northwestern University Evanston, Illinois 60201	1
Dr. B. Stanley Pons Department of Chemistry University of Alberta Edmonton, Alberta CANADA T6G 2G2	1
Dr. Michael J. Weaver Department of Chemistry Michigan State University East Lansing, Michigan 48824	1
Dr. R. David Rauh EIC Corporation 55 Chapel Street Newton, Massachusetts 02158	1
Dr. J. David Margerum Research Laboratories Division Hughes Aircraft Company 3011 Malibu Canyon Road Malibu, California 90265	1
Dr. Martin Fleischmann Department of Chemistry University of Southampton Southampton 509 5NH England	1
Dr. Janet Osteryoung Department of Chemistry State University of New York at Buffalo Buffalo, New York 14214	1
Dr. R. A. Osteryoung Department of Chemistry State University of New York at Buffalo Buffalo, New York 14214	1

TECHNICAL REPORT DISTRIBUTION LIST, 359

	No. Copies
Dr. Donald W. Ernst Naval Surface Weapons Center Code R-33 White Oak Laboratory Silver Spring, Maryland 20910	1
Dr. R. Nowak Naval Research Laboratory Code 6130 Washington, D.C. 20375	1
Dr. John F. Houlihan Shenango Valley Campus Pennsylvania State University Sharon, Pennsylvania 16146	1
Dr. D. F. Shriver Department of Chemistry Northwestern University Evanston, Illinois 60201	1
Dr. D. H. Whitmore Department of Materials Science Northwestern University Evanston, Illinois 60201	1
Dr. Alan Bewick Department of Chemistry The University Southampton, SO9 5NH England	
Dr. A. Himy NAVSEA-5433 NC #4 2541 Jefferson Davis Highway Arlington, Virginia 20362	
[illegible] Arnold Department of the Navy Strategic Systems Project Office Room 901 Washington, D.C. 20376	
Mr. James R. Moden Naval Underwater Systems Center Code 3632 Newport, Rhode Island 02840	1
Dr. Bernard Spielvogel U. S. Army Research Office P. O. Box 12211 Research Triangle Park, NC 27709	1
Dr. Denton Elliott Air Force Office of Scientific Research Bolling AFB Washington, D.C. 20332	1
Dr. David Aikens Chemistry Department Rensselaer Polytechnic Institute Troy, New York 12181	1
Dr. A. P. B. Lever Chemistry Department York University Downsview, Ontario M3J1P3 Canada	1
Dr. Stanislaw Szpak Naval Ocean Systems Center Code 6343 San Diego, California 95152	1
Dr. Gregory Farrington Department of Materials Science and Engineering University of Pennsylvania Philadelphia, Pennsylvania 19104	
Dr. Bruce Dunn Department of Engineering & Applied Science University of California Los Angeles, California 90024	

TECHNICAL REPORT DISTRIBUTION LIST, 359

	No. Copies
M. L. Robertson Manager, Electrochemical and Power Sonices Division Naval Weapons Support Center Crane, Indiana 47522	1
Dr. Elton Cairns Energy & Environment Division Lawrence Berkeley Laboratory University of California Berkeley, California 94720	1
Dr. Micha Tomkiewicz Department of Physics Brooklyn College Brooklyn, New York 11210	1
Dr. Lesser Blum Department of Physics University of Puerto Rico Rio Piedras, Puerto Rico 00931	1
Dr. Joseph Gordon, II IBM Corporation K33/281 5600 Cottle Road San Jose, California 95193	1
Dr. Robert Somoano Jet Propulsion Laboratory California Institute of Technology Pasadena, California 91103	1
Dr. Johann A. Joebstl USA Mobility Equipment R&D Command [illegible] [illegible] Virginia 22060	1
Dr. Judith H. Ambrus NASA Headquarters M.S. RTS-6 Washington, D.C. 20546	1
Dr. Albert R. Landgrebe U.S. Department of Energy M.S. 6B025 Forrestal Building Washington, D.C. 20595	1
Dr. T. Marks Department of Chemistry Northwestern University Evanston, Illinois 60201	1
Dr. D. Cipris Allied Corporation P. O. Box 3000R Morristown, New Jersey 07960	1
Dr. M. Philpot IBM Corporation 5600 Cottle Road San Jose, California 95193	1
Dr. Donald Sandstrom Washington State University Department of Physics Pullman, Washington 99164	1
Dr. Carl Kannewurf Northwestern University Department of Electrical Engineering and Computer Science Evanston, Illinois 60201	1
Dr. Edward Fletcher University of Minnesota Department of Mechanical Engineering Minneapolis, Minnesota 55455	1
Dr. John Fontanella U.S. Naval Academy Department of Physics Annapolis, Maryland 21402	1
Dr. Martha Greenblatt Rutgers University Department of Chemistry New Brunswick, New Jersey 08903	1
Dr. John Wassib Kings Mountain Specialties P. O. Box 1173 Kings Mountain, North Carolina 28086	1

TECHNICAL REPORT DISTRIBUTION LIST, 359

	No. Copies	No. Copies
Dr. J. J. Brophy University of Utah Department of Physics Salt Lake City, Utah 84112	1	
Dr. Walter Roth Department of Physics State University of New York Albany, New York 12222	1	
Dr. Thomas Davis National Bureau of Standards Polymer Science and Standards Division Washington, D.C. 20234	1	
Dr. Charles Martin Department of Chemistry Texas A&M University	1	
Dr. Anthony Sammells Institute of Gas Technology 3424 South State Street Chicago, Illinois 60616	1	
Dr. H. Tachikawa Department of Chemistry Jackson State University Jackson, Mississippi 39217	1	
Dr. W. M. Risen Department of Chemistry Brown University Providence, Rhode Island	1	